Purdue University
Purdue e-Pubs

Earth, Atmospheric, and Planetary Sciences Faculty Publications

Department of Earth and Atmospheric Sciences

1-1-2009

Characterizing heart rate variability by scale-dependent Lyapunov exponent

J Hu
Purdue University

J. Gao

W. Tung
Purdue University

Follow this and additional works at: http://docs.lib.purdue.edu/easpubs

Repository Citation

Hu, J; Gao, J.; and Tung, W., "Characterizing heart rate variability by scale-dependent Lyapunov exponent" (2009). *Earth, Atmospheric, and Planetary Sciences Faculty Publications.* Paper 2.
http://docs.lib.purdue.edu/easpubs/2

This document has been made available through Purdue e-Pubs, a service of the Purdue University Libraries. Please contact epubs@purdue.edu for additional information.

AIP | Chaos
An Interdisciplinary Journal of Nonlinear Science

Characterizing heart rate variability by scale-dependent Lyapunov exponent

Jing Hu, Jianbo Gao, and Wen-wen Tung

Citation: Chaos **19**, 028506 (2009); doi: 10.1063/1.3152007
View online: http://dx.doi.org/10.1063/1.3152007
View Table of Contents: http://chaos.aip.org/resource/1/CHAOEH/v19/i2
Published by the American Institute of Physics.

Related Articles

Four-dimensional ultrasound current source density imaging of a dipole field
Appl. Phys. Lett. 99, 113701 (2011)

Reentrant excitation in an analog-digital hybrid circuit model of cardiac tissue
Chaos 21, 023121 (2011)

Analysis of heart rate variability signal in meditation using second-order difference plot
J. Appl. Phys. 109, 114703 (2011)

Magnetocardiography with sensors based on giant magnetoresistance
Appl. Phys. Lett. 98, 153705 (2011)

A comparison of two-dimensional techniques for converting magnetocardiogram maps into effective current source distributions
Rev. Sci. Instrum. 82, 014302 (2011)

Additional information on Chaos

Journal Homepage: http://chaos.aip.org/
Journal Information: http://chaos.aip.org/about/about_the_journal
Top downloads: http://chaos.aip.org/features/most_downloaded
Information for Authors: http://chaos.aip.org/authors

ADVERTISEMENT

Downloaded 24 Feb 2012 to 128.210.124.59. Redistribution subject to AIP license or copyright; see http://chaos.aip.org/about/rights_and_permissions

Characterizing heart rate variability by scale-dependent Lyapunov exponent

Jing Hu,[1,2] Jianbo Gao,[1,a)] and Wen-wen Tung[3]
[1]*PMB Intelligence LLC, P.O. Box 2077, West Lafayette, Indiana 47996, USA*
[2]*Affymetrix, Inc., 3380 Central Expressway, Santa Clara, California 95051, USA*
[3]*Department of Earth and Atmospheric Sciences, Purdue University, West Lafayette, Indiana 47907, USA*

(Received 16 December 2008; accepted 18 May 2009; published online 30 June 2009)

Previous studies on heart rate variability (HRV) using chaos theory, fractal scaling analysis, and many other methods, while fruitful in many aspects, have produced much confusion in the literature. Especially the issue of whether normal HRV is chaotic or stochastic remains highly controversial. Here, we employ a new multiscale complexity measure, the scale-dependent Lyapunov exponent (SDLE), to characterize HRV. SDLE has been shown to readily characterize major models of complex time series including deterministic chaos, noisy chaos, stochastic oscillations, random $1/f$ processes, random Levy processes, and complex time series with multiple scaling behaviors. Here we use SDLE to characterize the relative importance of nonlinear, chaotic, and stochastic dynamics in HRV of healthy, congestive heart failure, and atrial fibrillation subjects. We show that while HRV data of all these three types are mostly stochastic, the stochasticity is different among the three groups. © *2009 American Institute of Physics*. [DOI: 10.1063/1.3152007]

Determining whether heartbeat dynamics is chaotic or stochastic is an important issue, both theoretically and clinically. The problem is difficult to solve neatly, however, since heart rate variability (HRV) may exhibit both nonlinear, and possibly chaotic, as well as stochastic behaviors. This motivates us to employ a recently developed multiscale complexity measure, the scale-dependent Lyapunov exponent (SDLE), to characterize HRV. SDLE cannot only unambiguously distinguish chaos from noise but also characterize various types of complex time series. Using SDLE, we are able to quantify the relative importance of nonlinear, chaotic, and stochastic dynamics in HRV of healthy, congestive heart failure, and atrial fibrillation subjects.

I. INTRODUCTION

Despite extensive studies on HRV using chaos theory,[1–10] fractal scaling analysis,[11–15] and many other methods in the last two decades, the issue of whether HRV is chaotic or stochastic remains highly controversial. The debate can hardly be settled if one does not go beyond the standard theories of chaos and random fractals, since the foundations for the two theories are different: chaos theory is mainly concerned about apparently irregular behaviors in a complex system that are generated by nonlinear deterministic interactions with only a few degrees of freedom, where noise or intrinsic randomness does not play an important role, while random fractal theory assumes that the dynamics of the system are inherently random.[16] To shed new light on the problem, here we employ a new multiscale complexity measure, the SDLE,[16,17] to characterize HRV, especially the relative importance of nonlinear, chaotic, and stochastic dynamics in HRV of healthy, congestive heart failure (CHF), and atrial fibrillation (AF) subjects.

II. HRV ANALYSIS BY SDLE

A. SDLE as a multiscale complexity measure

SDLE is defined in a phase space through consideration of an ensemble of trajectories.[16,17] In the case of a scalar time series $x(1),x(2),\ldots,x(n)$, a suitable phase space may be obtained by using time delay embedding[18–20] to construct vectors of the form

$$V_i=[x(i),x(i+L),\ldots,x(i+(m-1)L)], \tag{1}$$

where m and L are called the embedding dimension and the delay time, respectively. For chaotic systems, m and L have to be chosen according to certain optimization criterion.[16] For a stochastic process, which is infinite dimensional, the embedding procedure transforms a self-affine stochastic process to a self-similar process in a phase space, and often $m=2$ is not only sufficient but also best illustrates a nonchaotic scaling behavior from a finite data set.[16,17]

We now become more concrete. Denote the initial distance between two nearby trajectories by ε_0 and their *average* distances at time t and $t+\Delta t$, respectively, by ε_t and $\varepsilon_{t+\Delta t}$, where Δt is small. The SDLE $\lambda(\varepsilon_t)$ is defined by[16,17]

$$\varepsilon_{t+\Delta t}=\varepsilon_t e^{\lambda(\varepsilon_t)\Delta t} \quad \text{or} \quad \lambda(\varepsilon_t)=\frac{\ln \varepsilon_{t+\Delta t}-\ln \varepsilon_t}{\Delta t}, \tag{2}$$

or equivalently by

$$\frac{d\varepsilon_t}{dt}=\lambda(\varepsilon_t)\varepsilon_t \quad \text{or} \quad \frac{d\ln \varepsilon_t}{dt}=\lambda(\varepsilon_t). \tag{3}$$

To compute SDLE, we can start from an arbitrary number of shells,

[a)]Author to whom correspondence should be addressed. Electronic mail: jbgao@pmbintelligence.com. Telephone: +1 765-418-8025.

 © 2009 American Institute of Physics

Downloaded 24 Feb 2012 to 128.210.124.59. Redistribution subject to AIP license or copyright; see http://chaos.aip.org/about/rights_and_permissions

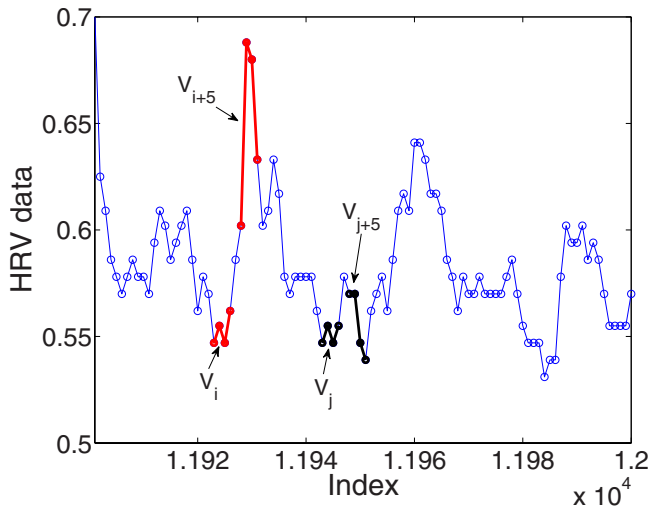

FIG. 1. (Color online) A schematic showing how the method is applied to HRV analysis.

$$\varepsilon_k \leq \|V_i - V_j\| \leq \varepsilon_k + \Delta\varepsilon_k, \quad k = 1,2,3,\ldots, \tag{4}$$

where V_i, V_j are reconstructed vectors and ε_k (the radius of the shell) and $\Delta\varepsilon_k$ (the width of the shell) are arbitrarily chosen small distances ($\Delta\varepsilon_k$ is not necessarily a constant). Then we monitor the evolution of all pairs of points (V_i, V_j) within a shell and take average. Equation (2) can now be written as

$$\lambda(\varepsilon_t) = \frac{\langle \ln\|V_{i+t+\Delta t} - V_{j+t+\Delta t}\| - \ln\|V_{i+t} - V_{j+t}\|\rangle}{\Delta t}, \tag{5}$$

where t and Δt are integers in unit of the sampling time and the angle brackets denote average within a shell. Figure 1 illustrates how the method is used to analyze HRV.

Note that the initial set of shells for computing SDLE serves as initial values of the scales; through evolution of the dynamics, they will automatically converge to the range of inherent scales. This is emphasized by the subscript t in ε_t—when the scales become inherent, t can then be dropped. Also note that when analyzing chaotic time series, the condition

$$|j - i| \geq (m-1)L \tag{6}$$

needs to be imposed when finding pairs of vectors within a shell, to eliminate the effects of tangential motions, and for an initial scale to converge to the inherent scales.[16]

At this point, it is important to note that SDLE is related to the finite-size Lyapunov exponent (FSLE).[21] However, there are important differences between the two metrics. The two major ones are that (1) FSLE is always positive while SDLE can be positive, zero, and negative and (2) SDLE is much easier to compute than FSLE.

To better understand SDLE, we now point out a relation between SDLE and the largest positive Lyapunov exponent λ_1 for a true chaotic signal. It is given by[16]

$$\lambda_1 = \int_0^{\varepsilon^*} \lambda(\varepsilon) p(\varepsilon) d\varepsilon, \tag{7}$$

where ε^* is a scale parameter (for example, used for renormalization when using the algorithm of Wolf *et al.*[22]), $p(\varepsilon)$ is the probability density function for the scale ε given by

$$p(\varepsilon) = Z\frac{dC(\varepsilon)}{d\varepsilon}, \tag{8}$$

where Z is a normalization constant satisfying $\int_0^{\varepsilon^*} p(\varepsilon)d\varepsilon = 1$, and $C(\varepsilon)$ is the well-known correlation integral of Grassberger–Procaccia.[23]

We now list three interesting scaling laws of SDLE that are most relevant to HRV analysis:

(1) For clean chaos on small scales and noisy chaos with weak noise on intermediate scales,

$$\lambda(\varepsilon) = \lambda_1. \tag{9}$$

To facilitate chaos analysis of HRV, we define chaos to be observing scaling of Eq. (9) on a scale range of $(\varepsilon, r\varepsilon)$, where $r > 1$ is a coefficient.[16,17,21] When low-dimensional chaos is concerned, one may require $r \geq 2$. Note that such a definition of chaos is able to detect chaos in intermittent time series with a long laminar phase during which neighboring trajectories do not diverge, and a rapid divergence over a small part of the state space, as well as chaos from time series with multiple positive Lyapunov exponents and very high dimension (say, more than 20). However, it should be noted that when the dimension of a signal is very high, the scale range for observing Eq. (9) could be very narrow.

(2) For clean chaos on large scales where memory has been lost and for noisy chaos (including chaos with measurement/dynamic noise and noise-induced chaos[24–26]) on small scales,

$$\lambda(\varepsilon) \sim -\gamma \ln \varepsilon, \tag{10}$$

where $\gamma > 0$ is a parameter. Recently, using an ensemble forecasting approach, we have proven (but not published yet) that $\gamma = D/D(\varepsilon_0)$, where D and $D(\varepsilon_0)$ are the information dimension on infinitesimal and an initial finite scale in ensemble forecasting. When a noisy data set is finite due to lack of data, D would soon saturate when m exceeds certain value. However, if the finite scale is quite large, $D(\varepsilon_0) \sim m$ for a wide range of m. Therefore, $\gamma \sim 1/m$ when m exceeds a certain value. This point will be further discussed through the context of HRV analysis.

(3) For random $1/f^{2H+1}$ processes, where $0 < H < 1$ is called the Hurst parameter which characterizes the correlation structure of the process: depending on whether H is smaller than, equal to, or larger than 1/2, the process is said to have antipersistent, short-range, or persistent long-range correlations,[16,27]

$$\lambda(\varepsilon) \sim \varepsilon^{-1/H}. \tag{11}$$

Note that the standard Brownian motion corresponds to $H = 1/2$ and generally $H < 1/2$ for HRV.[13–15]

Downloaded 24 Feb 2012 to 128.210.124.59. Redistribution subject to AIP license or copyright; see http://chaos.aip.org/about/rights_and_permissions

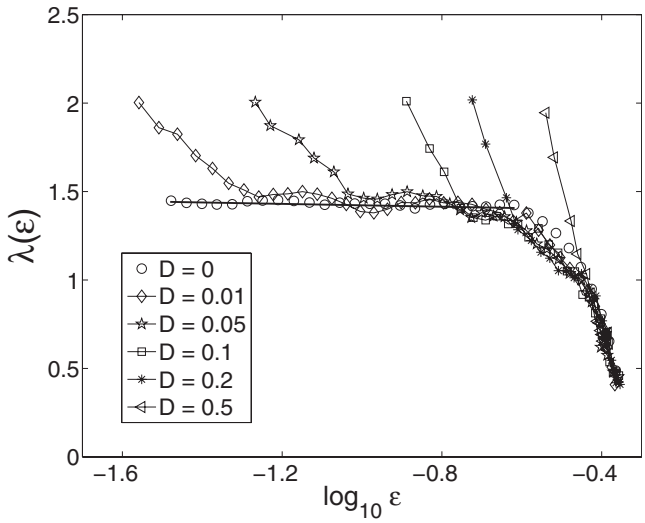

FIG. 2. $\lambda(\varepsilon)$ curves for the clean and the noisy Lorenz system with measurement noise.

Note that the scaling law of Eq. (10) or Eq. (11) alone does not indicate whether the time series under study is linear or nonlinear. However, there is a simple way to test for nonlinearity if the system under study is dissipative. The method involves calculating SDLE from the original and the time-order reversed time series, $x_n, x_{n-1}, \ldots, x_2, x_1$. When the system is dissipative, the SDLEs for the two time series are very different. This indicates that SDLE is another effective way to test for time irreversibility.[28–30]

It is helpful to illustrate the above scaling laws by using an example. For this purpose, let us examine the Lorenz system,

$$dx/dt = -16(x-y),$$
$$dy/dt = -xz + 45.92x - y, \tag{12}$$
$$dz/dt = xy - 4z.$$

Note that the system with dynamical noise was studied earlier.[16,17] To illustrate the similarities and differences of the effects of measurement and dynamical noise on SDLE, here we study measurement noise. For this purpose, we simply add a Gaussian white noise of zero mean and variance $D^2\sigma_0^2$ to the x-component of the system sampled with a time interval of 0.06, where $\sigma_0^2 \approx 167$ is the variance of the clean Lorenz data. The length of the time series is 10 000 and $m=4$, $L=2$. Figure 2 shows a number of curves corresponding to different D. We note that for the clean system, there are two scaling laws. One is Eq. (9), $\lambda(\varepsilon) \approx 1.48$, for small ε; the other is Eq. (10) for large ε where memory has been lost. For the noisy data, the scale region where the scaling law of Eq. (9) shrinks when noise is increased. While this feature is similar to that of dynamical noise, it is interesting to note two differences: (1) the largest resolvable SDLE with dynamical noise is about 2.5, but that with measurement noise is only about 2.0. Also, on small scales the scaling of Eq. (10) is less smooth than that of dynamical noise; (2) in the case of dynamical noise, parameter γ does not appear to depend on the noise strength. However, in the case of measurement noise, γ increases with the strength of noise. Note that distinguishing measurement from dynamical noise is an important but difficult issue.[31] The different behaviors of SDLE due to measurement and dynamical noise discussed here may be used to develop a practical scheme to help distinguish measurement from dynamical noise (in fact, an integral form of SDLE has been applied to estimate the strength of measurement and dynamical noise[32–34]). We shall carefully pursue this issue in the near future.

Finally, we illustrate how SDLE can deal with nonstationarity. When analyzing long HRV data sets, a common experience is that there are at least two types of nonstationarity: (1) sudden jumps or outliers, where some of the jumps are intrinsic to the system, while others may be caused by errors during measurement; (2) oscillatory components due to, for example, respiration. These nonstationarities often lead to poor fractal scaling of raw HRV data. Since $1/f$-type behavior is one of the most salient features of HRV, before we carry out an analysis of HRV using SDLE, it is important to first examine whether SDLE can meaningfully characterize $1/f$ processes perturbed by the two types of nonstationarity identified above. Specifically, we study the following two types of processes:

(1) Shift a $1/f^\beta$, $\beta=2H+1$ process downward or upward at randomly chosen points in time by an arbitrary amount. For convenience, we call this procedure type-1 nonstationarity and the processes obtained broken-$1/f^\beta$ processes.
(2) At randomly chosen time intervals, concatenate randomly broken-$1/f^\beta$ processes and oscillatory components or superimpose oscillatory components on broken-$1/f^\beta$ processes. This procedure causes a different type of nonstationarity, which for convenience we shall call type-2 nonstationarity.

We call the resulting random processes perturbed $1/f^\beta$ processes. A number of examples of the $\lambda(\varepsilon)$ curves for such processes, where the frequency of the perturbations is on average 1% of the simulated data, are shown in Fig. 3. We observe that Eq. (11) still holds very well when $\lambda(\varepsilon) > 0.02$. Therefore, SDLE can readily characterize $1/f$ processes perturbed by either of the nonstationarities identified.

To understand why the SDLE can deal with type-1 nonstationarity, it suffices to note that type-1 nonstationarity causes shifts in the trajectory in phase space; the greater the nonstationarity, the larger the shifts. The SDLE, however, cannot be affected much by shifts, especially large ones, since it is based on the coevolution of pairs of vectors within chosen small shells. In fact, the effect of shifts is to exclude a few pairs of vectors that were originally counted in the ensemble average. Therefore, so long as the shifts are not too frequent, the effect of shifts can be neglected, since ensemble average within a shell involves a large number of pairs of vectors.

Let us now turn to type-2 nonstationarity which involves oscillatory components. Being regular, oscillatory components can only affect $\lambda(\varepsilon)$ where it is close to 0. Therefore, type-2 nonstationarity cannot affect the positive portion of $\lambda(\varepsilon)$ either. Note that similar types of perturbations have

Downloaded 24 Feb 2012 to 128.210.124.59. Redistribution subject to AIP license or copyright; see http://chaos.aip.org/about/rights_and_permissions

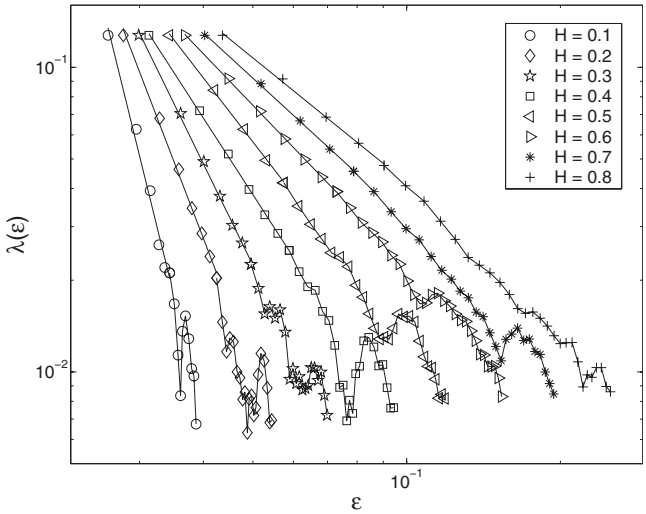

FIG. 3. $\lambda(\varepsilon)$ vs ε curves for perturbed $1/f$ processes. Eight different H are considered. To put all the curves on one plot, the curves for different H (except the smallest one considered here) are arbitrarily shifted rightward.

been carried out to clean and noisy chaotic data, and the major features of Eqs. (9) and (10) are also robust, as expected.

B. Analysis of HRV

We analyzed 15 HRV data sets downloaded from PhysioNet entitled, "Is the normal heart rate chaotic? Data for study," five each for healthy, CHF, and AF subjects. We used the original data instead of the data with outliers filtered out, since outliers do not affect calculation of SDLE, as we already have discussed. Being able to directly work on raw HRV data without any preprocessing is one of the merits of SDLE.

We have found (and will show momentarily) that HRV data are mostly stochastic in the sense that the scaling described by Eq. (9) is not observed in any significant scale range in any of the HRV data sets, no matter what embedding parameters are used. The noisy nature of HRV suggests that it is best to construct a phase space with $m=2$, $L=1$ when analyzing a finite data set. Below, we first discuss the general behaviors of SDLE for HRV of the three types of subjects, then summarize the effects of embedding parameters and data length on the behaviors of SDLE.

Figure 4(a1) illustrates the scaling of SDLE for HRV of healthy subjects in general. We clearly observe the scaling described by Eq. (10) on the smallest scales. When Fig. 4(a1) is replotted in log-log scale, as shown in Fig. 4(a2), we observe a linearlike relation on larger scales [corresponding to where $\lambda(\varepsilon)$ is slightly positive] with a Hurst parameter $H=1/6.93\approx 0.14$. Therefore, the dynamics of normal HRV also contain a $1/f$-like behavior described by the scaling of Eq. (11). Note that the scale range where Eq. (11) holds is necessary short since H here is very small (see also the two leftmost curves in Fig. 3).

The behavior of SDLE for HRV of CHF subjects is markedly different from that of normal HRV. A typical result is shown in Fig. 4(b1) in semilog scale. Note that the value of $\lambda(\varepsilon)$ is now much closer to zero and the pattern of $\lambda(\varepsilon)$ is

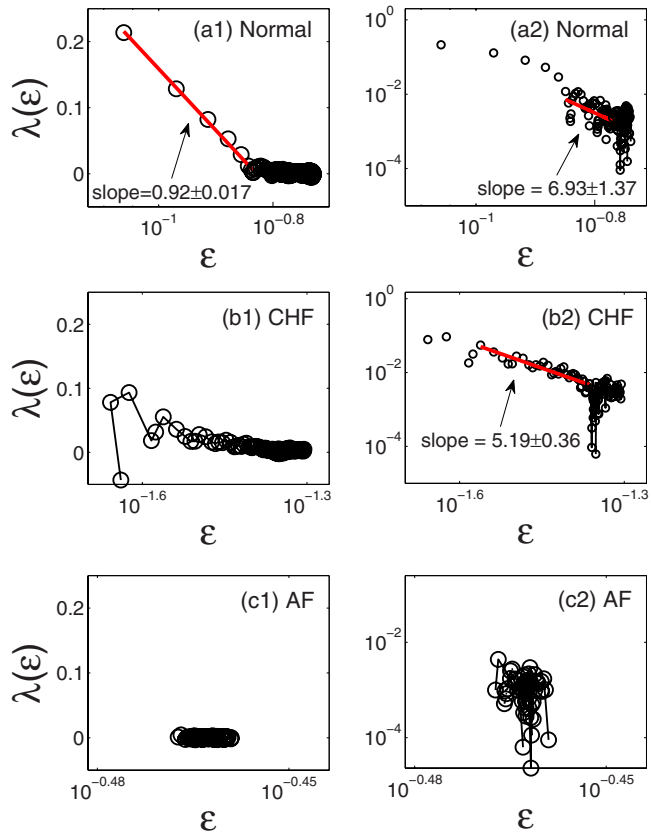

FIG. 4. (Color online) $\lambda(\varepsilon)$ curves for HRV of [(a1) and (a2)] normal, [(b1) and (b2)] CHF, and [(c1) and (c2)] AF subjects. Plots in the left panel are in semilog scale, while those in the right panel are in log-log scale. For better comparison, results for data sets n1rr.txt, c1rr.txt, and a3rr.txt are shown here since they have similar length (99 791, 75 543, and 85 304 points, respectively). The results are similar when only a part of these data is used.

somewhat oscillatory. Unable to resolve the dynamics on scales with $\lambda(\varepsilon)$ markedly different from zero is a signature of high-dimensional system.[16] Therefore, the dimension of HRV dynamics in CHF subjects is much higher than that in normal subjects. Note that this behavior is termed as a decrease in cardiac chaos in CHF patients.[10] When Fig. 4(b1) is replotted in a log-log scale, as shown in Fig. 4(b2), an approximate linear relation emerges almost on all scales. This suggests that HRV in CHF subjects behaves as a $1/f$ process described by Eq. (11). The slope in the figure gives a Hurst parameter $H=1/5.19\approx 0.19$. At this point, it should be emphasized that the pattern of SDLE in Figs. 4(a2) and 4(b2) is quite different from that of fractional Brownian motion (fBm) processes shown in Fig. 3. Two reasons may be that fBm processes are linear, monofractal random processes while HRV dynamics are nonlinear[10,35] and multifractal.[15]

Finally, we examine SDLE for HRV of AF patients. A representative result is shown in Figs. 4(c1) and 4(c2) in semilog and log-log scales, respectively [where the evolution time starts from $t>(m-1)L=1$]. Since we only observe $\lambda(\varepsilon)\approx 0$, we conclude that the dynamics in HRV of AF subjects are like white noise. This suggests that the dimension of HRV of AF subjects is the highest among the three groups.

Finally, we summarize the effects of embedding dimension and data length on calculating SDLE from HRV (following general practice, we fix $L=1$; in fact, different L does

Downloaded 24 Feb 2012 to 128.210.124.59. Redistribution subject to AIP license or copyright; see http://chaos.aip.org/about/rights_and_permissions

not change much the results). (1) With fixed embedding parameters, for a long HRV data set, SDLE curves corresponding to different shells defined by Eq. (4) often do not collapse on one another but are parallel; similarly, the scaling of Eq. (10) may shift horizontally when the data length changes. However, γ remains quite stable. (2) For a data set of finite fixed length, when the embedding dimension m becomes bigger, the scale range defining the scaling of Eq. (10) becomes shorter; also, as pointed out when discussing Eq. (10), γ is roughly inversely proportional to m when m is large. Both features suggest that the scaling of Eq. (10) no longer becomes well defined when a finite length time series is embedded to a too high-dimensional phase space. (3) The scaling of Eq. (11), while becoming less well defined when a data set becomes shorter, is independent of the embedding dimension. This ought to be so. Otherwise, H becomes meaningless.

The effect (1) above warrants an explanation. To understand it, we first recall that the scale ε_t is the distance between two embedding vectors, $\varepsilon_t = \|V_{i+k} - V_{j+k}\|$, where $t = k\delta t$ and δt is the sampling time. Now suppose we have a stationary time series $\{x_i\}$. We split it into two segments of equal length. We then multiply all the elements in the second segment by a constant $a > 1$ and denote the resulting two segments by $\{y_i\}$ and $\{z_i\}$. The overall time series now has become nonstationary. It is obvious that ε in the space constructed by $\{y_i\}$ and $\{z_i\}$ also differs by a factor a, and the scaling of Eq. (10) for $\{y_i\}$ and $\{z_i\}$ will also be separated by a factor of a. Interestingly, both scalings of Eq. (10) for $\{y_i\}$ and $\{z_i\}$ will be captured, since our algorithm involves a series of initial shells defined by Eq. (4). Therefore, the parallel shifting of scaling Eq. (10) for HRV of different data length and corresponding to different shells suggests that the scaling of Eq. (10) is an inherent property of HRV, and that HRV is usually nonstationary.

III. CONCLUDING REMARKS

To shed new light on determining whether HRV is chaotic or stochastic, in this paper, we have employed SDLE to characterize HRV. We have not observed the chaotic scaling described by Eq. (9) on any significant scale ranges from any of the HRV data sets. Therefore, the HRV data analyzed here do not possess the defining property of standard chaos theory—truly exponential divergence between nearby trajectories in a phase space. Instead, we find that the dynamics in HRV of healthy subjects are characterized by scalings of Eqs. (10) and (11) on different scale ranges, and the dynamics of HRV in CHF patients are mostly like $1/f$ processes, while that in AF patients are like white noise.

In the literature, based on entropy measures on certain fixed scales (say, 15% or 20% of the standard deviation of the data),[1–3] it is often concluded that normal HRV is more complex than CHF HRV, since the entropy values on average are larger for normal HRV. Extending such an argument to SDLE, one would have to reach the same conclusion, since the largest value of SDLE for normal HRV is typically larger than that for CHF HRV. One even has to conclude that AF HRV is the least complex. We do not think this is the case for the following reasons. (1) The results based on entropy measures could change if a different scale (say, 3% of the standard deviation) is chosen. Such a behavior has indeed been observed with SDLE. (2) The inference that AF HRV is the least complex is simply inconsistent with the fact that AF HRV is like white noise, and hence, has the largest entropy. These considerations and the relation between the small scale behavior of SDLE and dimension of the data compel us to think that the greater difficulty in resolving scaling of Eq. (10) in CHF and AF subjects implies that the dimension of HRV increases from normal to CHF to AF and suggests that a healthy cardiovascular system is a tightly coupled system with coherent functions, while components in a malfunctioning cardiovascular system are somewhat loosely coupled and function incoherently, and thus need more variables to fully describe the dynamics.

ACKNOWLEDGMENTS

This work is partially supported by NSF (Grant No. CMMI-0825311).

[1] J. S. Richman and J. R. Moorman, Am. J. Physiol. Heart Circ. Physiol. **278**, H2039 (2000).
[2] S. M. Pincus and R. R. Viscarello, Obstet. Gynecol. **79**, 249 (1992).
[3] M. Costa, A. L. Goldberger, and C. K. Peng, Phys. Rev. E **71**, 021906 (2005).
[4] D. T. Kaplan and A. L. Goldberger, J. Cardiovasc. Electrophysiol. **2**, 342 (1991).
[5] A. L. Goldberger and B. J. West, Ann. N.Y. Acad. Sci. **504**, 195 (1987).
[6] J. K. Kanters, N. H. Holstein-Rathlou, and E. Agner, J. Cardiovasc. Electrophysiol. **5**, 591 (1994).
[7] M. Osaka, K. H. Chon, and R. J. Cohen, J. Cardiovasc. Electrophysiol. **6**, 441 (1995).
[8] M. Costa, I. R. Pimentel, T. Santiago, P. Sarreira, J. Melo, and E. Ducla-Soares, J. Cardiovasc. Electrophysiol. **10**, 1350 (1999).
[9] L. Glass, J. Cardiovasc. Electrophysiol. **10**, 1358 (1999).
[10] C. S. Poon and C. K. Merrill, Nature (London) **389**, 492 (1997).
[11] M. Kobayashi and T. Musha, IEEE Trans. Biomed. Eng. **29**, 456 (1982).
[12] J. T. Bigger, R. C. Steinman, L. M. Rolnitzky, J. L. Fleiss, P. Albrecht, and R. J. Cohen, Circulation **93**, 2142 (1996).
[13] C. K. Peng, J. Mietus, J. M. Hausdorff, S. Havlin, H. E. Stanley, and A. L. Goldberger, Phys. Rev. Lett. **70**, 1343 (1993).
[14] Y. Ashkenazy, P. C. Ivanov, S. Havlin, C. K. Peng, A. L. Goldberger, and H. E. Stanley, Phys. Rev. Lett. **86**, 1900 (2001).
[15] P. C. Ivanov, L. A. N. Amaral, A. L. Goldberger, S. Havlin, M. G. Rosenblum, Z. R. Struzik, and H. E. Stanley, Nature (London) **399**, 461 (1999).
[16] J. B. Gao, Y. H. Cao, W. W. Tung, and J. Hu, *Multiscale Analysis of Complex Time Series: Integration of Chaos and Random Fractal Theory, and Beyond* (Wiley, New York, 2007).
[17] J. B. Gao, J. Hu, W. W. Tung, and Y. H. Cao, Phys. Rev. E **74**, 066204 (2006).
[18] N. H. Packard, J. P. Crutchfield, J. D. Farmer, and R. S. Shaw, Phys. Rev. Lett. **45**, 712 (1980).
[19] F. Takens, in *Dynamical Systems and Turbulence*, Lecture Notes in Mathematics Vol. 898, edited by D. A. Rand and L. S. Young (Springer-Verlag, Berlin, 1981), p. 366.
[20] T. Sauer, J. A. Yorke, and M. Casdagli, J. Stat. Phys. **65**, 579 (1991).
[21] M. Cencini, M. Falcioni, E. Olbrich, H. Kantz, and A. Vulpiani, Phys. Rev. E **62**, 427 (2000).
[22] A. Wolf, J. B. Swift, H. L. Swinney, and J. A. Vastano, Physica D **16**, 285 (1985).
[23] P. Grassberger and I. Procaccia, Phys. Rev. Lett. **50**, 346 (1983).
[24] J. B. Gao, S. K. Hwang, and J. M. Liu, Phys. Rev. Lett. **82**, 1132 (1999).
[25] J. B. Gao, C. C. Chen, S. K. Hwang, and J. M. Liu, Int. J. Mod. Phys. B **13**, 3283 (1999).
[26] K. Hwang, J. B. Gao, and J. M. Liu, Phys. Rev. E **61**, 5162 (2000).
[27] J. B. Gao, J. Hu, W. W. Tung, Y. H. Cao, N. Sarshar, and V. P. Roychowdhury, Phys. Rev. E **73**, 016117 (2006).

Downloaded 24 Feb 2012 to 128.210.124.59. Redistribution subject to AIP license or copyright; see http://chaos.aip.org/about/rights_and_permissions

[28]M. Costa, A. L. Goldberger, and C. K. Peng, Phys. Rev. Lett. **95**, 198102 (2005).
[29]C. Diks, J. C. Vanhouwelingen, F. Takens, and J. Degoede, Phys. Lett. A **201**, 221 (1995).
[30]L. Stone, G. Landan, and R. M. May, Proc. R. Soc. London, Ser. B **263**, 1509 (1996).
[31]M. Strumik, W. M. Macek, and S. Redaelli, Phys. Rev. E **72**, 036219 (2005).
[32]J. Hu, J. B. Gao, and K. D. White, Chaos, Solitons Fractals **22**, 807 (2004).
[33]J. B. Gao, Physica D **106**, 49 (1997).
[34]C. J. Cellucci, A. M. Albano, P. E. Rapp, R. A. Pittenger, and R. C. Josiassen, Chaos **7**, 414 (1997).
[35]G. Q. Wu, N. M. Arzeno, L. L. Shen, D. K. Tang, D. A. Zheng, N. Q. Zhao, D. L. Eckberg, and C. S. Poon, PLoS ONE **4**, e4323 (2009).

Downloaded 24 Feb 2012 to 128.210.124.59. Redistribution subject to AIP license or copyright; see http://chaos.aip.org/about/rights_and_permissions